JOURNAL OF MATERIALS SCIENCE **37** (2002) 3867–3874

The black layer underneath the anode of dc-biased silver metaphosphate glass

A. DOI, H. MORIKAWA
Department of Materials, Nagoya Institute of Technology, Nagoya 466-8555, Japan
E-mail: akiradoi@mse.nitech.ac.jp

M. TAZAWA
National Institute of Advanced Industrial Science and Technology, Chubu, Nagoya 463-8687, Japan

The black layer was generated underneath the anode when a gold-electroded silver metaphosphate glass, a silver-ion conductor, was dc biased with 500 V/cm or 250 V/cm at 140°C . It was concluded that this layer corresponded to the silver-depleted region formed by conduction of the silver ions towards the cathode. The blackening was ascribed to be due to the shortened Ag-O distance, caused by structural rearrangement within the region into the P_2O_5-like structure on biasing.

1. Introduction

The silver metaphosphate ($AgPO_3$) glass is a silver-ion conductor. Electrolysis of this glass proceeded [1] when a sample with deposited gold on both sides was biased with ∼500 V/cm at ∼140°C (some 20°C below the glass transition temperature [2]). The features associating with the electrolysis are varied:

(i) The silver ions conducted towards and accumulated underneath the cathode, and pushed up the cathode above the glass surface.

(ii) Some of the silver ions which reached the cathode penetrated through it, were neutralized on the outermost surface, and changed the color of the cathode surface to silver.

(iii) Some of the silver ions which were neutralized at the cathode oozed out radially on the glass surface from the circular gold cathode, and formed the silver dendrites.

(iv) In the bulk, the silver dendrites grew from the cathode towards the anode, especially from the edge of the cathode to the edge of the anode.

(v) Some of the gold ions in the gold anode were injected into glass and penetrated to some extent, say, to several thousand Å.

(vi) The silver-depleted region (or more generally the positive-ion depleted region (PDR)) developed underneath the anode by conduction of the silver ions.

(vii) The black layer was generated underneath the anode, with thickness of ∼10 μm or more. This layer was not generated when silver in place of gold was used as the anode.

(viii) Many of the samples biased with 500 V/cm or higher showed the bubbles on the anode surface, possibly by evolution of the oxygen gas. Oxygen accumulation was seen at the anode-glass interface [1].

The purpose of the present work was to gain insight into the nature of the black layer formed. Emphasis was given on the comparison between this layer and the PDR.

2. Experimental

The samples were made by melting a mixture of appropriate amounts of $NH_4H_2PO_4$ and $AgNO_3$ in a platinum crucible at 500°C for 1–2 h in air, quenching on a carbon plate to a thickness of ∼0.5 mm, and depositing the gold electrodes of ∼1 cm^2 in area and 500–1400 Å in thickness on both sides.

The samples were then dc biased with single or multiple (50 ms of biasing followed by 50 ms of off-biasing) pulses of 500 V/cm or 250 V/cm at 140°C for 10 s *in vacuo*. The induced current, i, was detected as an output voltage, V_o ($=iR_r$), across a reference resistor R_r ($=1.18\Omega$) by an oscilloscope. After the dc run, the depth profiles of gold, silver, oxygen, and phosphorus were measured from the electrode surfaces with an x-ray photoelectron spectroscopy (XPS), after intermittent etchings of the surface with argon ions. Since the etching rate was different for different compositions and different materials, as well as for variable experimental settings, the sputtering time rather than the depth was used as the abscissa. By our XPS apparatus we could measure the profiles to the depth ∼1 μm, but not further. Therefore, some samples were cleaved and the cross sections were surveyed with an electron-probe microanalysis (EPMA) and a scanning electron microscope (SEM).

In order to study the black layer optically, the electrodes were removed and the absorbance was measured in the frequency range of 200–800 nm. After biasing a sample with dc voltage, the gold anode became erasible by rubbing with an ethanol-soaked cotton gauze,

but not so for the gold cathode. So, we polished away the cathode by using diamond slurry.

3. Results

Fig. 1 shows the response curves of samples I and II to 500 V/cm biasing with single or multiple pulses, respectively. As mentioned previously [3], the current at the onset of biasing, $i(t \rightarrow 0)$, corresponds to the dc conductivity of our glass at 140°C, $\sim 2 \times 10^{-4}$ S/cm. The current rise thereafter was ascribed [1] to the conductivity rise by joule heating, and the following decline to the formation of a resistive layer by depletion of the charge carriers. No noticeable differences in the overall response curves were found between the samples dc biased with single or multiple pulses.

For 500 V/cm-biased samples the charges flowed during biasing, Q(on), lie within 0.4–0.6 C/cm^2. The PDR thicknesses were estimated to be 1.7–2.6 μm and the thicknesses of the silver layers depositing beneath the cathode 0.43–0.64 μm, on the assumptions that no silver ions exist in the PDR and that the same amount of the silver ions accumulate onto the cathode, to give Q(on).

Fig. 2 shows the depth profiles on both sides of sample II after 500 V/cm biasing, with Q(on) of 0.48 C/cm^2. The ratios of number of atoms for silver to phosphorus, Ag/P, and oxygen to phosphorus, O/P, are plotted in Fig. 3, on the assumption that the phosphorus atoms are immobile on biasing. Except in the very proximity of the anode, the ratio of number of atoms of oxygen to phosphorus was invariable irrespective of the polarity of the electrode. Fig. 4 shows the ratios of number of atoms of Ag, P, and O on the anode side, [+], to those on the cathode side, [−], with the starting point in the abscissa being chosen at respective ends of the sputtering time. Therefore, the plots are only

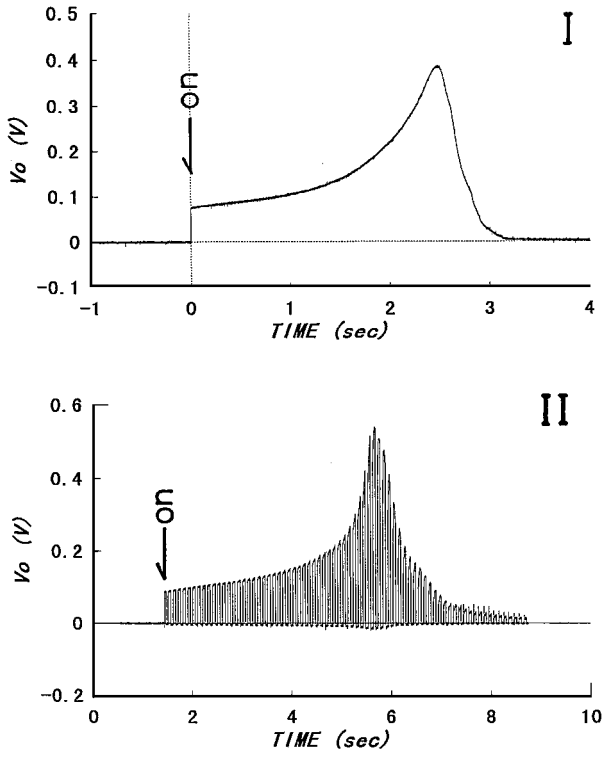

Figure 1 Electrical responses of samples I and II to 500 V/cm biasing with single or multiple pulses for 10 s, respectively.

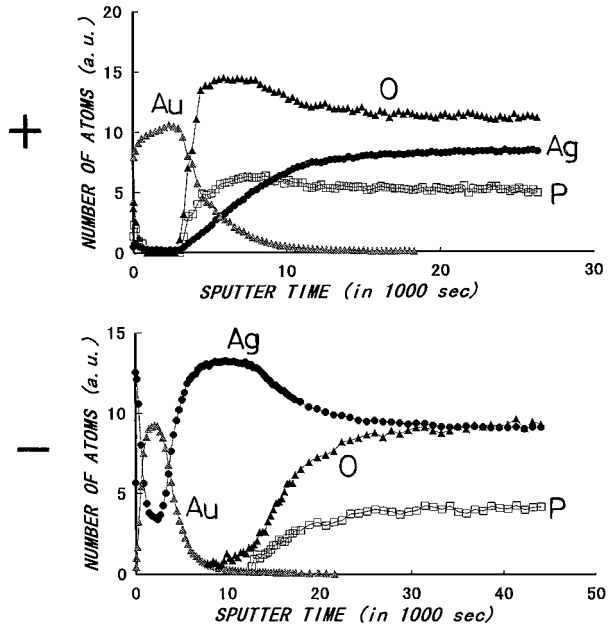

Figure 2 Depth profiles on the positive (+) and negative (−) sides of sample II after 500 V/cm biasing.

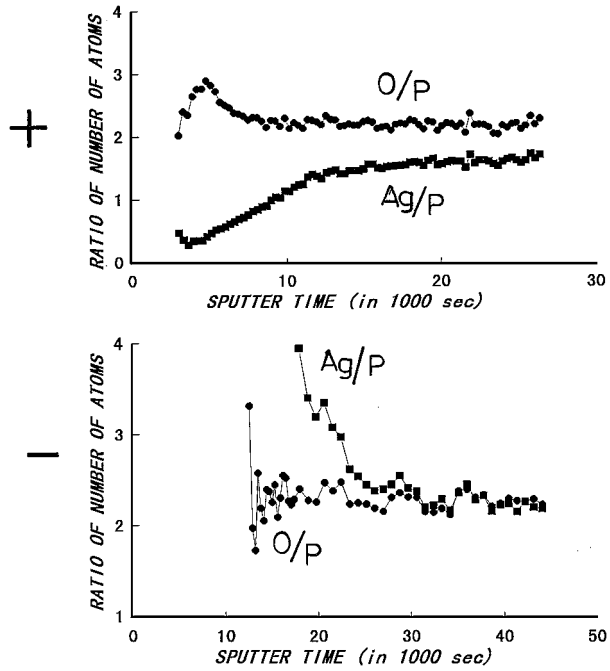

Figure 3 The ratios of number of atoms for oxygen to phosphorus, O/P, and silver to phosphorus, Ag/P, on the positive (+) and negative (−) sides of sample II as a function of the sputtering time.

qualitative, verifying that the silver ions are poor in concentration and phosphorus and oxygen rich in near parallel in the proximity of the anode.

Fig. 5 shows the EPMA line spectra of Ag, P, and O from the anode surface of sample III after 500 V/cm biasing, where Q(on) = 0.21 C/cm^2. (This sample was one of those polished on both sides of the as-quenched glasses for which Q(on) was reduced to 0.2–0.3 C/cm^2 by the polishing effect. A precise report on this topic will be given in a separate paper.) The dashed line indicates the end of the black layer, $\sim$19 μm thick, seen in the SEM image (Fig. 6) as well as by an optical microscope. That is, it seems that the black layer corresponds to the PDR itself.

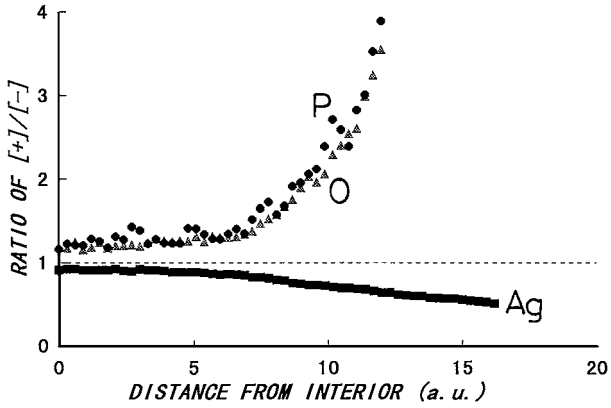

Figure 4 The ratios of number of atoms of Ag, P, and O on the anode side, [+], to those on the cathode side, [−], as a function of the distance from the interior towards the surface. The starting point in the abscissa was chosen at respective ends of the sputtering time (Fig. 2).

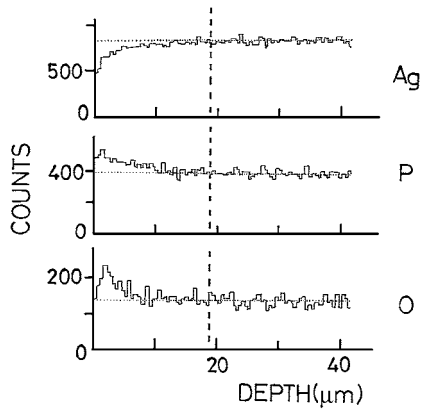

Figure 5 EPMA line spectra of Ag, P, and O on the anode side of sample III after 500 V/cm biasing. The dashed line represents the end of the black layer seen by the SEM.

A schematic illustration of the structure of the $AgPO_3$ glass, Fig. 7, is derived from the studies on alkali metaphosphate glass [4–10] as well as on the $AgPO_3$ crystal [11]. It is known [4] that the XPS O1s band shows the chemical shift due to the bridging oxygen

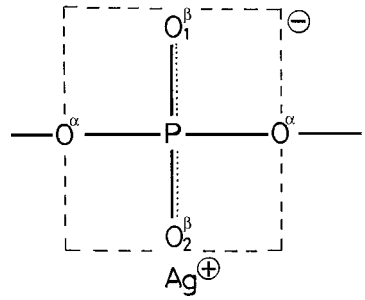

Figure 7 Schematic illustrating the structure of $AgPO_3$ glass suggested [4–11]. The oxygen atoms are classified into O^{α} and O^{β} because of the difference in the binding energy. The dots indicate the resonance effect due to π-bonding orbitals.

(O^{α}) and the nonbridging oxygen (O^{β}) when they compose the phosphate glass. Fig. 8 shows the observed O1s bands in the virgin glass and on the surface of the black layer of sample III, respectively. Because of identical distances of P-O_1^{β} and P-O_2^{β} it is suggested [4, 7] that there should be the resonance effect, as indicated by the dots in Fig. 7.

Fig. 9 shows the absorption coefficient of a virgin glass, and the absorbance of the black layer, respectively. In order to isolate absorption by the black layer, the absorbance of 500 V/cm-biased sample IV (which was almost identical in various aspects with sample II) *minus* absorbance of a virgin glass was plotted as a function of photon energy. The black layer gives broad absorption in the visible range.

Next, the experiment of polarity-reversal was made on the cell Au(A)/glass/Au(B). This sample V was biased with 250 V/cm for 10 s with Au(A) positive, followed by polarity-reversal after 5 min of interval, now with Au(B) positively biased. This experiment was done on the expectation that the black layer, formed underneath the Au(A) electrode in the first step of biasing, would be erased by the incoming silver ions in the second step of biasing provided the black layer is the PDR itself. In actuality, the black layers were formed on both sides.

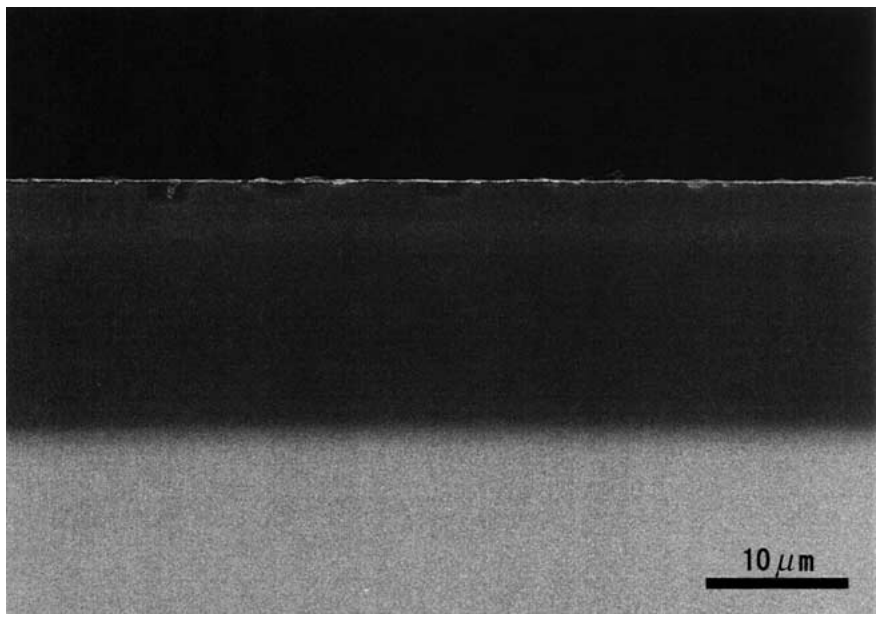

Figure 6 SEM image of the black layer, seen for sample III after 500 V/cm biasing.

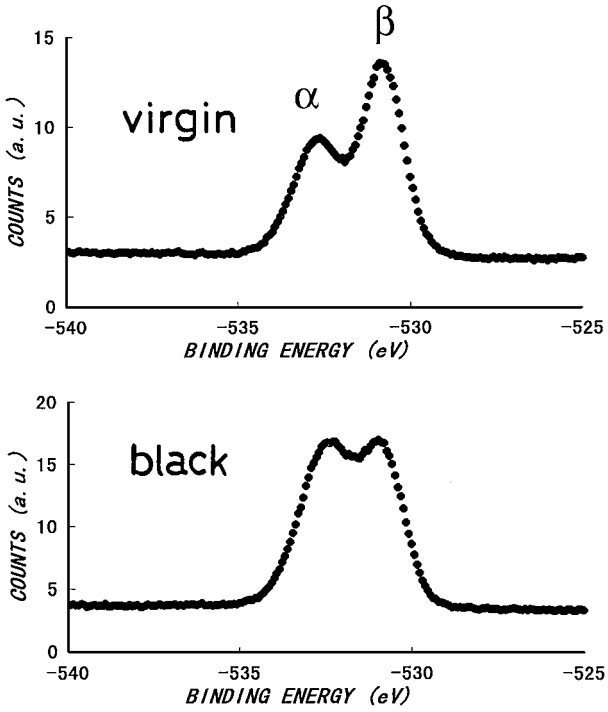

Figure 8 Chemical splitting of the XPS O1s band into two (α and β) in the virgin glass ("virgin") and in the black layer of sample III ("black").

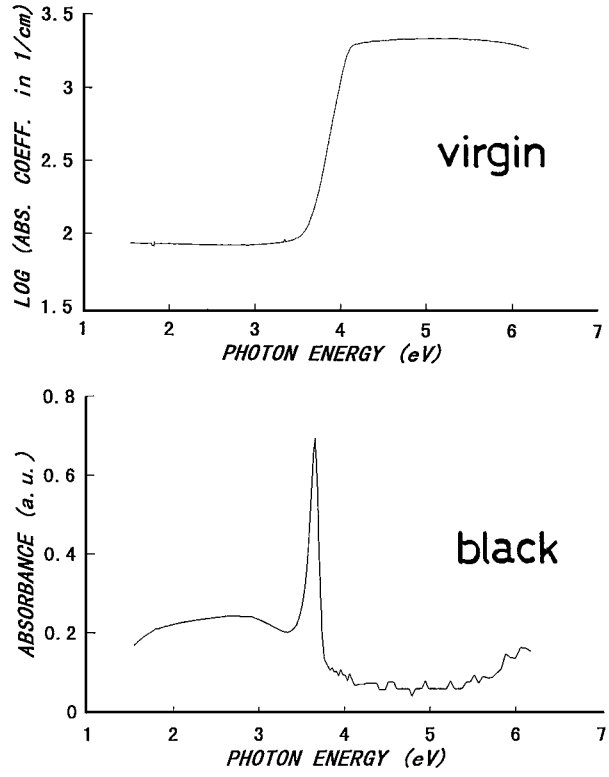

Figure 9 Absorption coefficient of a virgin glass ("virgin") and the difference in absorbances between the virgin glass and sample IV after 500 V/cm biasing ("black").

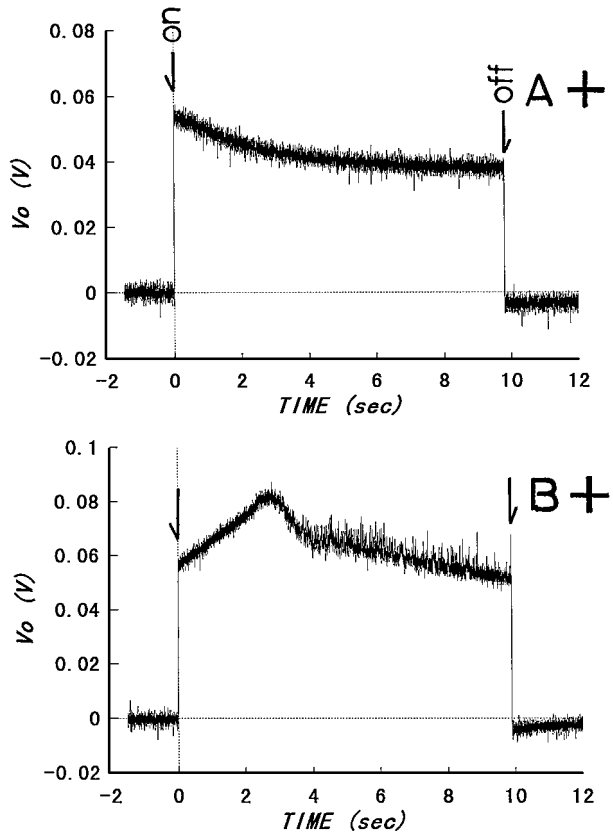

Figure 10 Electrical responses of sample V, in the configuration Au(A)/glass/Au(B), to 250 V/cm biasing with Au(A) positively biased ("A+"), followed by polarity-reversal now with Au(B) positively biased ("B+") after 5 min of interval.

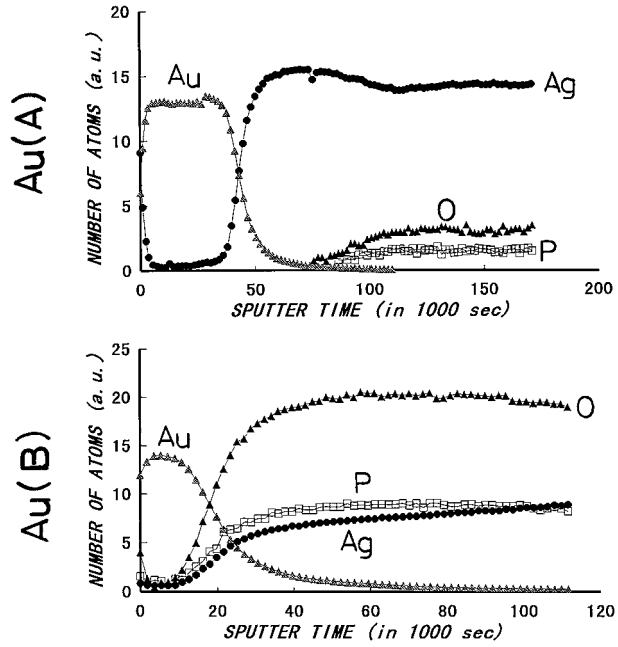

Figure 11 Depth profiles on Au(A) and Au(B) sides of sample V after sequential biasings with 250 V/cm (Fig. 10).

Fig. 10 shows the response curves of sample V. Contrary to 500 V/cm biasing (Fig. 1), 250 V/cm biasing induced steady current fall with time. On polarity-reversal, the current initially rose to the maximum, followed by the decline. This trend was what previously was observed on the sodium diborate glass [12]. The charge flowed on biasing, Q(on), was 0.22 C/cm^2 on Au(A) positive, and 0.33 C/cm^2 on Au(B) positive, respectively.

Fig. 11 shows the depth profiles on both sides after the sequence of dc biasings. The compositions at the end of the sputtering time (about 0.2 μm in depth) were $Ag_{10.0}P_{1.0}O_{2.4}$ on the Au(A) side, and $Ag_{1.1}P_{1.0}O_{2.3}$ on the Au(B) side. (It is to be noted that the composition of

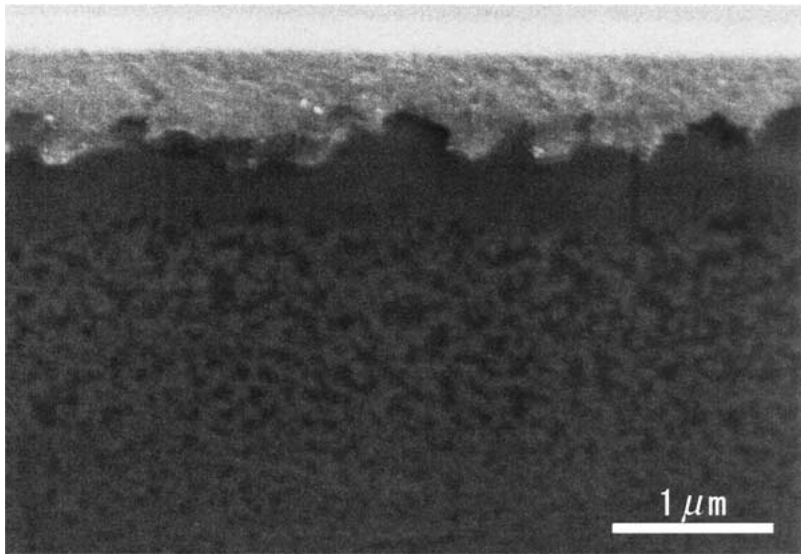

(A)

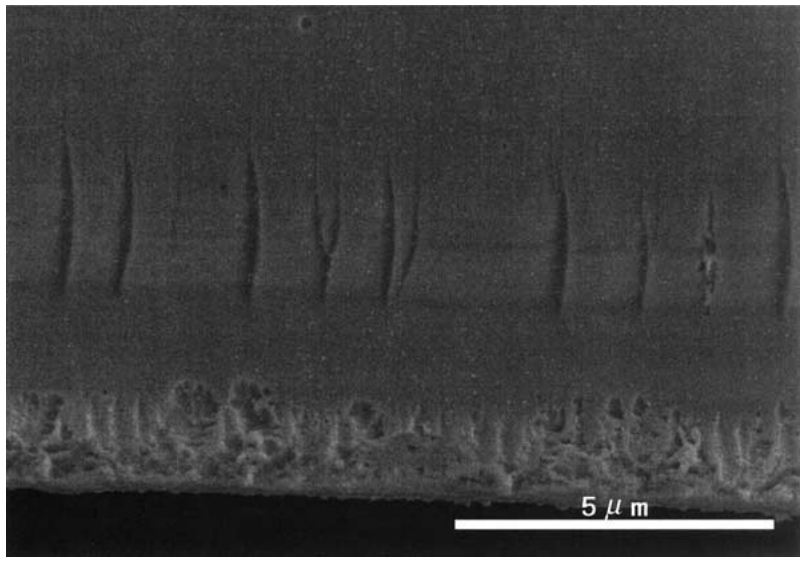

(B)

Figure 12 SEM images on the Au(A) side, (A), and Au(B) side, (B), of sample V after sequential biasings with 250 V/cm (Fig. 10).

a virgin glass by XPS was $Ag_{1.1}P_{1.0}O_{3.4}$. We are uncertain at present why oxygen was poor on both sides of the dc-biased samples studied so far). The SEM image on the Au(A) side (Fig. 12) shows the deposited silver layer with width 0.3–0.7 μm. Therefore, the richness in silver and the poornesses in oxygen and phosphorus at the end of the sputtering time on the Au(A) side (Fig. 11) means that the XPS data were still from within the deposited silver layer, although encompassing the data from the glassy phase. The charge flowed in the second step, 0.33 C/cm^2, corresponds to the silver thickness of 0.35 μm. This is in rough accord with the observation.

However, the EPMA line spectra on the Au(A) side (Fig. 13) demonstrate depletion of silver and accumulations of phosphorus and oxygen within the black layer (the width of which, 7.8 μm, was obtained from the SEM image), in a similar way as for the depth profiles on the anode side of a single-pulsed sample (Fig. 5). The charge Q(on) estimated from the depleted silver ions, 0.19 C/cm^2, was comparable to 0.22 C/cm^2 which flowed on initial biasing. This implies that the black layer (or the PDR) formed on initial dc biasing would remain intact on the second (polarity-reversed) dc biasing.

Fig. 14 shows the EPMA line spectra on the Au(B) side. Contrary to those on the Au(A) side, the depletion of silver and accumulations of phosphorus and oxygen were poor. On initial biasing, the estimated width of the deposited silver underneath the Au(B) cathode was 0.23 μm. On biasing with Au(B) positive, those deposited silver atoms would first be injected into glass. Only after exhaustion of the deposited silver would the black layer be formed underneath the Au(B) anode. This may be the reason for poor depletion of silver and poor accumulations of phosphorus and oxygen on the Au(B) side. The SEM image on the Au(B) side (Fig. 12) shows the complex features. The features seen within 1.6 μm from the Au(B) anode may be the "exuviae" of the previously deposited silver.

For sample V the SEM image of the deposited silver layer was irregular (Fig. 12). However, this was not so for the samples biased with 250 V/cm for 10 s only once. The SEM image on the cathode side of sample VI (Fig. 15) reveals columnar deposition of silver, with

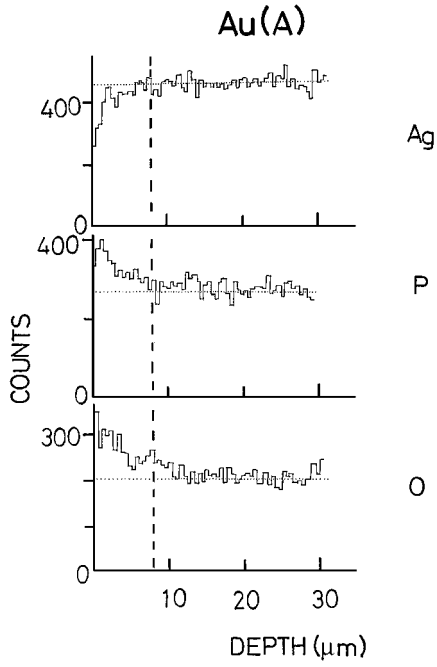

Figure 13 EPMA line spectra of Ag, P, and O on the Au(A) side of sample V after sequential biasings with 250 V/cm (Fig. 10). The dashed line represents the end of the black layer seen by the SEM.

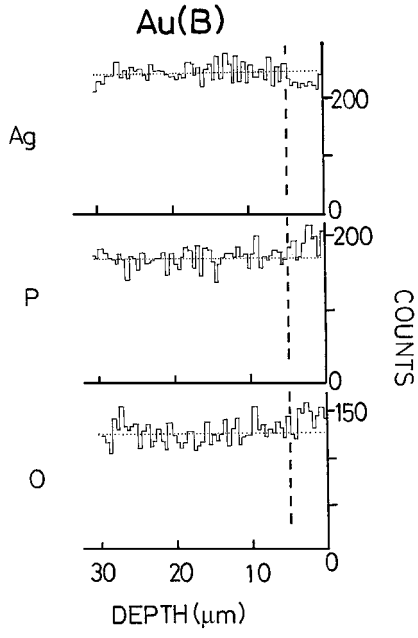

Figure 14 EPMA line spectra of Ag, P, and O on the Au(B) side of sample V after sequential biasings with 250 V/cm (Fig. 10). The dashed line represents the end of the black layer seen by the SEM.

the columns of ~30 nm in diameter and 0.31 μm in length. Compare this with the estimated width of the deposited silver layer from the charge flowed, 0.22 μm. Also formed on the cathode side were the "bullets" of unknown origin, lining up towards the anode (Fig. 15).

4. Discussion

The most noteworthy are the findings that the width of the black layer coincided well with the width of the PDR, and that silver depletion was quite incomplete, with deeper depletion in the proximity of the anode. The charge the depleted silver ions would give on their conduction, as estimated from the EPMA line spectrum, can be said to be comparable with the observed (Q(on)) in view of rough EPMA data involved.

Concerning incomplete depletion of silver, it is suggested that it arises from the presence of two types of the charge carriers in ion-conducting glass; namely, those who are able to conduct and another who are localized due to microheterogeneous nature of the glass structure. On dc biasing, those silver ions residing along the conduction paths would conduct first, to give the shallow and wide PDR. On further biasing, especially when the voltage drop across the PDR becomes noticeable, even those localized ions would become conducting and give the deeply depleted region in the very proximity of the anode.

Also found in the EPMA (Fig. 5) as well as in the XPS (Figs 2–4) spectra are the accumulations, in near parallel, of phosphorus and oxygen within the black layer. The SEM image of the black layer (Fig. 6) was darkened by the richnesses in oxygen and phosphorus and the poorness in silver within the layer, since the secondary-electron yield increases with atomic numbers. The glass structure (Fig. 7) as well as the observed near parallelism in the depth profiles of phosphorus and oxygen suggests that the cluster ions PO_3^- can be the dominant negative charge-carrying counterpart of the silver ions, besides or even more than the O_β^{2-} ions. In short, the depth profiles (Figs 2–5) demonstrate that the dominant effects of dc biasing are the conductions (and the accompanying accumulations/depletions at the electrode-glass interfaces) of the silver ions towards the cathode and the PO_3^- (and O_β^{2-}) ions towards the anode.

In an early stage of the work the black layer was considered to be related to the field-injected gold ions from the gold anode. However, the black layer was too thick (more than 10 μm) and the observed width of injected gold ions too thin, say, in several thousand Å (Fig. 2). Furthermore, the Au^+ ions and the Au^o atoms give the absorption bands mainly in the UV, while the $(Au^o)_n$ colloids in glass at 2.2–2.3 eV [13, 14]. On the other hand, the Ag^+ ions give the absorption bands in the UV, the Ag^o atoms give the sharp peak at 3.9 eV, and the $(Ag^o)_n$ colloids at 3.0–3.2 eV [15, 16]. Therefore, it seems at a glance of Fig. 9 that the sharp peak at 3.6–4.2 eV (depending on the samples) may be due to the Ag^o atoms. The truth is that this peak is an artefact, caused by saturation of an absorption coefficient (α) at photon energies above 4 eV (Fig. 9) by the detectability limit of our apparatus. The absorption edge (i.e., the band gap) of a virgin glass was estimated from the $(\alpha h\nu)^{1/2}$ versus $h\nu$ plots [17] (Fig. 16) to be 3.7 eV. The confusion arose from accidental coincidence in energies of the absorption edge and of the Ag^o band.

The shape of the O1s band was different between the virgin glass and the black layer (Fig. 8). Gaussian deconvolution of the band reveals that the ratio of number of atoms for O^α/O^β was 0.64 for the virgin glass while 1.3 for the black layer. Since the ideal values of the ratio are 0.5 for the $AgPO_3$ glass and 1.5 for the P_2O_5 glass [4], it is suggested that the composition of the black layer may be similar to that of the P_2O_5 glass. The IR

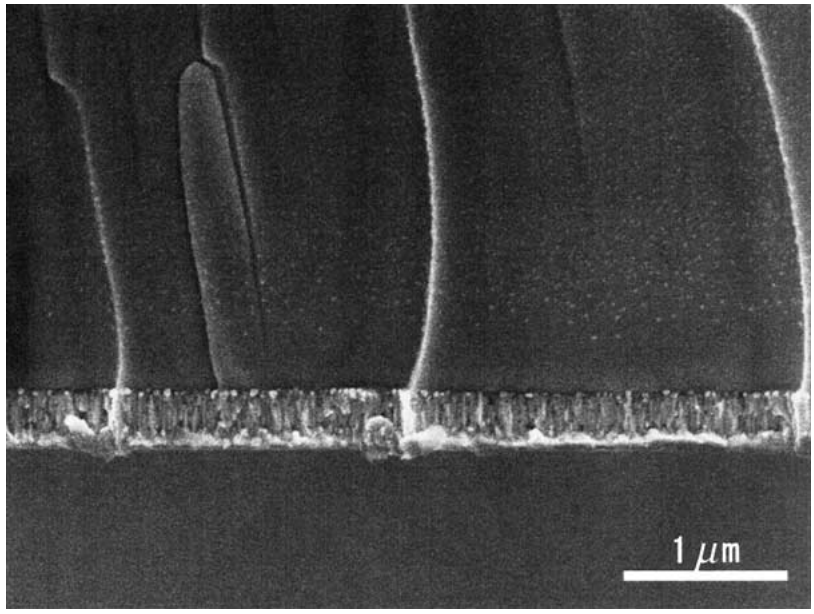

(A)

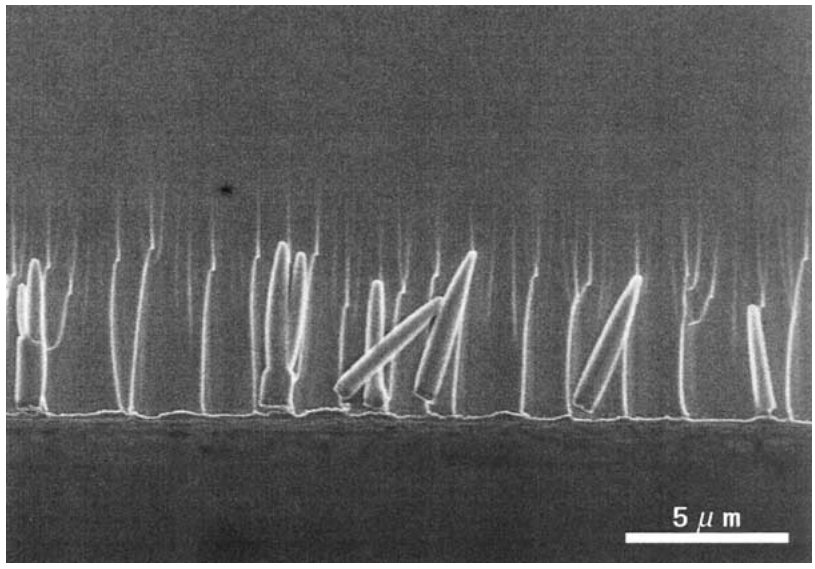

(B)

Figure 15 SEM images on the cathode side of sample VI after biasing with 250 V/cm for 10 s only once. (A) is for the fragment of the sample after washing supersonically with acetone, and (B) for the as-cloven fragment. By washing the majority of the "bullets" dropped out.

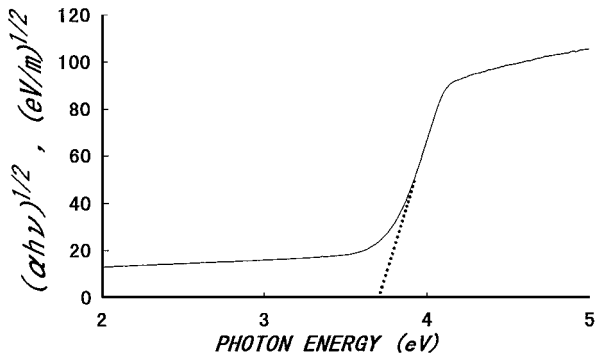

Figure 16 The plot of $(\alpha h\nu)^{1/2}$ versus photon energy, $h\nu$, for the virgin glass in Fig. 9. The dots, as extrapolated from the linear portion, give the absorption edge of 3.7 eV.

study on the dc-biased alkali lead silicate glass [18] demonstrates that the reflection spectrum of the PDR resembles that of the silica glass. This is in accord with our observation. However, the structural rearrangement within the PDR seems not to be uniform. The O1s bands in the depth profiles of sample II (Fig. 2) were deconvoluted, to give the ratio of number of atoms for O^{α}-to-O^{β} as a function of the sputtering time (Fig. 17). It is apparent that the smaller the number of depleted silver ions with depth (Fig. 5), the closer was the ratio for O^{α}/O^{β} to that of a virgin glass.

From the above discussion it is suggested that the black layer is the PDR itself. A supporting evidence is no observation of the black layer when silver in place of gold was used as the anode [1], since the injected silver ions inhibit formation of the PDR. The blackening is caused by optical absorption in the visible range. The study of the irradiation effects on the phosphate glass [19] shows the appearance of the radiation-induced centers, the PO_4^- hole centers, absorbing in the visible to UV range. We are uncertain at present whether our color centers giving the black color are related to those radiation-induced centers or not.

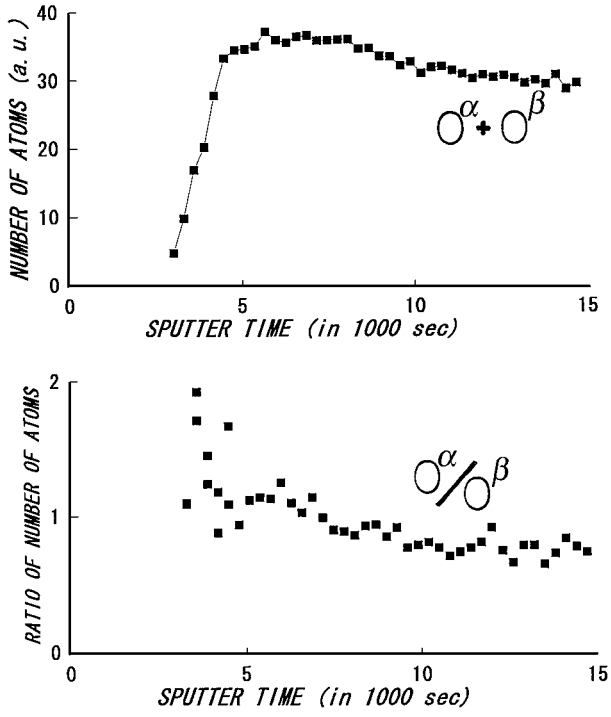

Figure 17 Comparison of the depth profile of oxygen on the anode side of sample II with the ratio of number of atoms for O^{α}/O^{β}.

However, the observed absorption is too broad, spanning the whole visible range, to be related to the color centers by imperfections. The blackening may rather be related to the Ag-O bond length. It is reported [20] that, in silver salts, the band gap decreases with a decreasing Ag-O distance, i.e., with increasing Ag-O bond strength. The shorter the Ag-O distance, the greater the 4d-5s hybridization of the Ag^{+} ions and the smaller is the band gap between the 4d-like valence band and the 5s-like conduction band. If a silver salt contains the Ag-O distance shorter than 2.26 Å, the color is black [20]. Then, it is possible that the blackening appears as a result of structural rearrangement within the PDR, by which the Ag-O distance may be reduced to below 2.26 Å. The aforementioned inability of erasing the black layer formed underneath the Au(A) electrode on the subsequent polarity-reversal (Figs 10–14) favors this hypothesis.

5. Conclusions

When a gold-electroded silver metaphosphate glass was dc biased with 500 V/cm or 250 V/cm at 140°C, the black layer was generated underneath the anode. This layer was not seen when silver in place of gold was used as the anode. Several techniques were employed to characterize this layer. It was concluded that this layer corresponded to the positive-ion depleted region (PDR) formed underneath the anode by conduction of the silver ions towards the cathode. The depletion was quite incomplete, however, spanning over many microns in width. In addition to silver depletion, accumulations of phosphorus and oxygen were seen within the PDR. It is suggested that the cluster ions PO_3^- are the dominant negative charge-carrying counterpart of the silver ions in our glass.

The blackening of the PDR is assigned, tentatively, to be due to the shortened Ag-O distance to less than 2.26 Å, caused by structural rearrangement within the PDR into the P_2O_5-like structure on biasing. The black layer remained intact when the electrode (underneath which the black layer was formed when it acted the anode) changed its role into the cathode on the second dc biasing. This intactness may also be the result of structural rearrangement within the PDR.

References

1. A. DOI and N. ASAKURA, *J. Mater. Sci.* **36** (2001) 3897.
2. M. MANGION and G. P. JOHARI, *Phil. Mag.* B **57** (1988) 121.
3. A. DOI, H. TAKANO and H. TAKAKI, *J. Appl. Phys.* **86** (1999) 2655.
4. R. GRESCH, W. MÜLLER-WARMUTH and H. DUTZ, *J. Non-Cryst. Solids* **34** (1979) 127.
5. K. SUZUKI and M. UENO, *J. Phys. (Paris)* C **8** (1985) 261.
6. R. K. BROW, R. J. KIRKPATRICK and G. L. TURNER, *J. Non-Cryst. Solids* **116** (1990) 39.
7. U. HOPPE, G. WALTER and D. STACHEL, *Phys. Chem. Glasses* **33** (1992) 216.
8. J. SWENSON, A. MATIC, A. BRODIN, L. BÖRJESSON and W. S. HOWELLS, *Phys. Rev.* B **58** (1998) 11331.
9. T. UCHINO and T. YOKO, *J. Non-Cryst. Solids* **263/264** (2000) 180.
10. R. K. BROW, *ibid.* **263/264** (2000) 1.
11. K. H. JOST, *Acta Crystallogr.* **14** (1961) 779.
12. A. DOI, *Solid St. Ionics* **109** (1998) 279.
13. W. A. WEYL, *J. Phys. Chem.* **57** (1953) 753.
14. I. TANAHASHI and T. TOHDA, *J. Amer. Ceram. Soc.* **79** (1996) 796.
15. R. YOKOTA and K. SHIMIZU, *J. Phys. Soc. Jpn.* **12** (1957) 833.
16. U. KREIBIG, *Appl. Phys.* **10** (1976) 255.
17. N. F. MOTT and E. A. DAVIS, "Electronic Processes in Non-Crystalline Materials" (Oxford University Press, 1979).
18. D. E. CARLSON, K. W. HANG and G. F. STOCKDALE, *J. Amer. Ceram. Soc.* **57** (1974) 295.
19. D. L. GRISCOM, E. J. FRIEBELE, K. J. LONG and J. W. FLEMING, *J. Appl. Phys.* **54** (1983) 3743.
20. H. Y.-P. HONG, J. A. KAFALAS and J. B. GOODENOUGH, *J. Solid St. Chem.* **9** (1974) 345.

Received 29 October 2001
and accepted 25 April 2002